



Eco-Friendly Formulation of Selenium Nanoparticles and Its Functional Characterization against Breast Cancer and Normal Cells

Srinivasan Rajasekar¹ · Santhi Kuppusamy²

Received: 22 May 2020 / Published online: 8 August 2020
© Springer Science+Business Media, LLC, part of Springer Nature 2020

Abstract

In the recent years, targeted cancer therapy induced by nanoparticles has been more effective than other treatment options; in addition, the green formulation of metal or non-metallic nanoparticles are of tremendous concern due to appreciation therapeutic performance with low toxicity to mammalian cells. Here, we reported eco-friendly formulation of selenium nanoparticles (SeNPs) achieved by biological route utilizing the *Carica papaya* latex. The UV–Visible Spectrophotometer (UV–Vis) analysis, Fourier-transform infrared spectroscopy (FT-IR), X-ray powder diffraction (XRD), dynamic light scattering (DLS), and Transmission electron microscopy (TEM) analysis were used to confirm the SeNPs formation. MTT assay proved its biological properties such as anti-cancer efficacy against the cultured MDA-MB-231 cells. The findings showed that MDA-MB-231 cells were severely impacted by the green synthesized SeNPs as compared with the normal HBL100 cell line. The IC₅₀ value of green synthesized SeNPs toward MDA-MB-231 cells was noted to be 34 µg/mL for 48 h, while HBL-100 cells showed no cytotoxic effects at concentrations as high above 50 µg/mL for 48 h over SeNPs. Our finding indicates that the delivery of biosynthesized SeNPs has a greater clinical efficiency for MDA-MB-231 breast cancer cells.

Keywords Selenium nanoparticle · *Carica papaya* latex · Breast cancer · MDA-MB-231 cells

Introduction

Nanotechnology and Nanoscience describes the study and implementation of nanoscale materials in different scientific disciplines, namely physics, chemistry, medicine, biology etc. [1, 2]. Emerging nanotechnology is an exciting emphasis on the use of nanoparticles in different range from 0.1 nm to 1000 nm, which promises a novel paradigm to early diagnosis and invention of infectious illnesses such as with cancer therapy [3]. The use of nanomaterials with different characteristics such as size, surface chemistry, morphology, surface charge and surface distribution may reflect their physicochemical properties and about their pharmacological importance appropriately [4]. Because of

their high surface area, nanoparticles have an enhanced catalytic potential and can produce reactive oxygen species (ROS) that cause higher toxic effect towards cancer cells [5].

Cancer is a vast group of diseases that can begin in almost any organ or tissue of the body because once abnormal cells grow uncontrollably, they invade neighboring parts of the body and/or spread to the other organs leading to death from cancer. Cancer is the second rising cause of death worldwide, causing an estimated 9.6 million deaths in 2018, or one in six deaths [6]. The most common forms of cancer in women are breast, lung, cervical, thyroid and colorectal cancer. Cancer has emerged as a significant threat and includes over 100 forms of cancer that define a causing different of defective cells have the ability to metastasize to other parts of the body. The global cancer economy is expected to reach \$150 Billion in 2020 [7].

Metal and metal oxide nanoparticles can be produced using various techniques, including physical, chemical and biological methods. Metal nanoparticles have been extensively examined throughout biomedical research because

✉ Srinivasan Rajasekar
sekarbioline@gmail.com

¹ Kathir Institute of Health Science Wisdom Tree,
Neelambur, Coimbatore, Tamil Nadu 641062, India

² Department of Botany, Selvamm Arts and Science College,
Namakkal, Tamil Nadu 637003, India

of their unusual, flexible physical and chemical characteristics. In contrast, due to its unique interaction with light, metal nanoparticles have a component means of monitoring the nano-complex therapeutic carriers within the body, allowing for a more efficient therapy with a decreased risk of adverse effects relative to traditional therapies. Electrostatic charge, surface chemistry and photothermal activity of the metal nanoparticles potentiate therapeutic effectiveness toward cancerous cells regardless of their high drug payload [8, 9]. Conventional physical and chemical approaches for the preparing of metallic nanoparticles have many issues and challenges, such as the application of organic toxic substances, by-products of reduction agents, multiple phase processes and a substantial intensity of protective agents needed for the colloidal stabilization of NPs, which can poses significant environmental and biological concerns [10].

Biological approach-based synthesis of metal and metal oxide NPs represents a groundbreaking path in the field of nanomedicine due to its usability, cost effectiveness and eco-friendliness. Nanobiotechnological studies such as NP formulation using biological components can be classified as “gold biotechnology” [11]. Various biologically active compounds, such as sugars, microorganisms, vitamins, biopolymers etc. can also be used as a raw material to produce metal and metal oxide NPs. These NPs synthesized via green methods use various parts of plant extract consisting of enzymes, proteins, flavonoids, terpenoids and cofactors that serve as reducing and capping agents [12–14]. Therefore, it is important to extend green chemistry concepts to nanotechnology where NPs will benefit from a greener approach that promotes both efficiency and safety. Emerging plant-mediated nanoparticles are reasonably fast, as compared with other biological systems has no need to establish different media and culture conditions. In particular, the fabrication of the metal and metal oxide NPs requires secondary metabolites such as phenolic acid, flavonoids, alkaloids, and terpenoids that naturally occur in various medicinal plants [15, 16]. Such secondary metabolites are used in redox reactions for formulating environmentally safe nanosize materials. The synthesis of metallic NPs has drawn significant interest due to their unique optical, chemical, electrical and magnetic properties. Selenium (Se) is a metalloid that belonging to group 16 of the periodic table and also is an important micronutrient in the human body as a cofactor for glutathione peroxidases and thioredoxine reductases, as well as playing a role in the develop immune system, cancer prevention as well as antioxidant and antiviral activity [17, 18]. Se is one of the key trace elements, essential nutritionally for the functioning of living cells of mammals and higher animals. Its plays a vital part in cancer treatment and immune response and its depletion in human body associated with cardiovascular diseases and

immune dysfunction. In-vivo, Se mainly exists as diverse selenoproteins, which play a crucial role in different functions such as cellular redox regulation, detoxification, and defense of immune-system [19, 20]. Increased concentrations of Se are harmful to the body cells, (upwards 400 $\mu\text{g}/\text{day}$), yet usually needed in adults between 10 and 20 mg, the recommended daily dietary allowance is 55 $\mu\text{g}/\text{day}$ [15, 21, 22]. In addition, Se insufficient will lead to immune system damage, and expanded potential for growth of emerging cancers. Owing to their remarkable bioavailability, biological activity, and lower toxicity of SeNPs have recently drawn much interest [23].

Selenium nanoparticles (SeNPs) are considered better to other metal nanoparticles, such as silver, gold and platinum NPs, due to their superior biocompatibility and superior in vivo degradability [24, 25]. In addition, SeNPs demonstrated other benefits, such as regulated size, potent drug load efficiency, increased antitumor activity and lower toxicity to normal cells. SeNPs are considered a major topic, along with their lesser side effects, due to its antiviral, antibacterial and antioxidant activity. Several in vitro and in vivo studies have shown that SeNPs disclose outstanding antioxidant capacity through progressively establishing selenoenzymes that remove free radicals within the body [16, 26]. Papaya (*Carica papaya* L.) is a tropical plant with a wealthy nutritional value and a considerably extraordinary product of carotenoids, provitamin A, α -tocopherol, ascorbate (vitamin C) and folates (vitamin B9) [27]. *Papaya latex* is a thixotropic liquid that has a milky appearance and comprises around 85% water. However, the soluble fraction possesses both biomolecules and the usual ingredients, include salts ($\sim 10\%$), carbohydrates ($\sim 10\%$), lipids ($\sim 5\%$), cysteine proteinases ($\sim 30\%$) and glutathione. *Carica papaya latex* is a milky white liquid composed of secondary metabolites and shows molluscicidal, antibacterial, insecticidal, antitumor, anti-fungal, inflammatory and antimutagenic activities [28, 29].

In the current research, we have synthesized Selenium nanoparticles (SeNPs) mediated by *Carica papaya latex*. Then, the UV–Vis, FTIR, XRD, DLS and TEM confirmed the formation of SeNPs and their cytotoxicity was examined against both normal (HBL-100) and cell type of breast cancer (MDA-MB-231). Finally, the apoptotic and anti-apoptotic protein expression were testified in SeNPs treated MDA-MD-231 cells.

Materials and Methods

Materials

The human MDA-MB-231 breast cancer cell line was purchased from National Center for Cell Science (NCCS,

Pune). Selenious acid (H_2SeO_3), MTT 3-(4, 5-dimethylthiazol 2-yl)-2, 5-diphenyltetrazolium bromide, 4',6-diamidino-2-phenylindole (DAPI), acridine orange/ethidium bromide (AO/EtBr), and sodium dodecyl sulphate (SDS) were purchased from Sigma Aldrich, India. All the reagents were used without further purification. Analytical grade reagents were purchased from Sigma-Aldrich (Bangalore, India). All the samples were prepared in Milli-Q water.

Collection of Latex

Carica papaya latex was extracted from the green fruits which were collected directly from trees in the Karuppur region, Salem District, Tamil Nadu, India. Locally grown *C. papaya* was used to collect fresh latex. Initially 4 to 6 longitudinal incisions 2 to 3 mm deep were made on the unripe mature fruit surface from fruit stalk end to the tip of the fruit by using a sharp stainless-steel knife in the early mornings (7.00–8.00 a.m.), as the flow of latex is low during the day. The latex that emerged after incision only lasted 1 to 2 min, then coagulated quickly and was stored in a glass container. All the aqueous solutions were prepared using double distilled water.

Synthesis of Se nanoparticles

In the standard reaction mixture, 5 mL of *C. papaya* latex was diluted to 50 mL using double distilled water and then 10 mL of latex solution was taken from this mixture with 20 mL of 40 mM aqueous selenious acid solution. The reaction product was stirred for 24 h at room temperature. After 24 h the resulting product was centrifuged at 15,000 rpm for 10 min. The pellet was washed with double distilled water and dried in vacuum. The powder form of the latex was used for further analysis.

Characterization of Selenium Nanoparticles

Several spectrophotometric techniques such as UV–visible Spectroscopy, Fourier Transformed Infrared Spectroscopy (FTIR), X-Ray Diffraction (XRD), Dynamic Light Scattering (DLS), and microscopic Transmission Electron Microscopy (TEM) characterized the biosynthesized SeNPs. TEM samples were prepared by putting a reduction in the suspension of NP on carbon-coated copper grids. The images on a JEOL JEM 2100 TEM electron microscope were visualized at 200 kV. On a Zeta sizer Nano ZS particle analyser (Malvern), the size distribution and surface charge on the SeNPs were determined in a suspension. UV visible spectroscopy (Shimadzu UV-1800) confirmed the formation of SeNP's. FTIR (Thermo Scientific NICOLET 5700) studies in the range of 500 cm^{-1} to 4000 cm^{-1} were

performed to determine the functional groups and the X-ray diffraction spectroscopy (Rigaku miniflex II X-ray diffractometer) was carried out at a voltage of 45 kV with Cu-K_α radiation ($\lambda = 1.5406\text{ \AA}$) to examine the crystalline phase of synthesized nanoparticles.

Cell Lines and Cell Culture

Human MDA-MB-231 breast cancer cells were collected from the National Center for Cell Science, Pune, India and stored in DMEM media enriched with 10% FBS, 1% L-glutamine, 1% penicillin, and 1% streptomycin stock solution, at $37\text{ }^\circ\text{C}$ and 5% CO_2 . The medium was modified every two days and the cells were transferred by trypsinization prior to confluence [30–32].

Cell Viability Assay

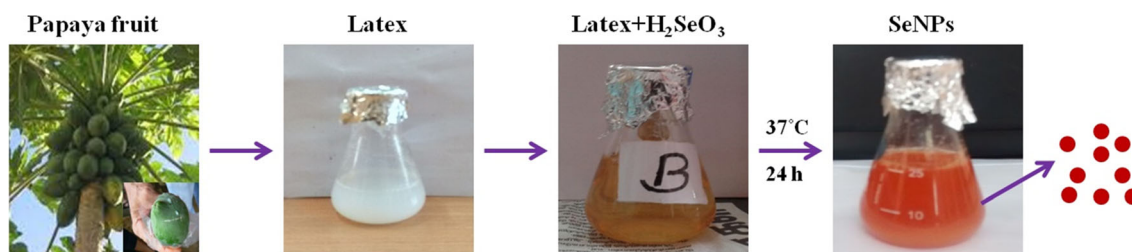
MTT assay was used to assess cell viability. The MDA-MB-231 cells were seeded in a 96-well plate at 5000 cells per line and incubated for 48 h. Cells were handled for 48 h with various concentrations of SeNPs (0, 10, 15, 20, 25, 30, 35, 40, 45, and $50\text{ }\mu\text{L/mL}$). The MTT, a tetrazolium salt, is converted by mitochondrial dehydrogenases in live cells into insoluble formazan. Formazan was dissolved and absorbance measured on an ELISA plate spectrophotometer (Bio Tek Instruments, Winooski, Vermont) at double wavelengths of 550 nm and 630 nm. This estimated the average number of viable cells compared to untreated test cells.

DAPI and AO/EtBr Staining

The experimental cells were grown in 6-well plate (2×10^6 cells/well), treated with SeNPs for 48 h and stained with DAPI. In addition, these cells were also treated with $3\text{ }\mu\text{g/mL}$ of AO/EtBr, washed with PBS and examined with a fluorescence microscope (FLoidTM Cell Imaging Station, THERMO FISHER).

Statistical Analysis

The data were seen in the parallel experiments as mean value \pm standard deviation (SD). Statistical analyses have been made using the Student's t test. $P < 0.05$ was considered important. Bio-Rad image analysis system with image-Pro software processing (Bio-Rad laboratories Inc., Hercules, CA, USA) was used to determine the width of the bands on the membrane.



Scheme 1 Schematic illustration of the biosynthesized SeNPs prepared from *Carica papaya* latex (color figure online)

Results and Discussion

Synthesis and Characterization of Selenium Nanoparticles

The schematic preparation reveals the SeNPs nanoparticles synthesized without any chemical reducing agents and was extracted efficiently from *Carica papaya* latex (Scheme 1). The presence of ruby red color noted SeNPs synthesis through an eco-friendly method and characterized by UV–

visible spectrophotometer, Fourier Transform Infrared Spectroscopy (FTIR), X-Ray Diffraction (XRD), Dynamic Light Scattering (DLS), Zeta Potential and Transmission Electron Microscopy (TEM). The presence of ruby red at the end of the incubation period (24 h) revealed the synthesis of SeNPs in aqueous solution, which (Fig. 1a) showed a typical SeNP UV–Vis spectrum with an absorption spectrum showing a strong peak at 277.5 nm and the observation of such band was assigned to Surface Plasmon Resonance (SPR) of the SeNPs particles. Once 40 mM selenious acid was applied to the solution, the color

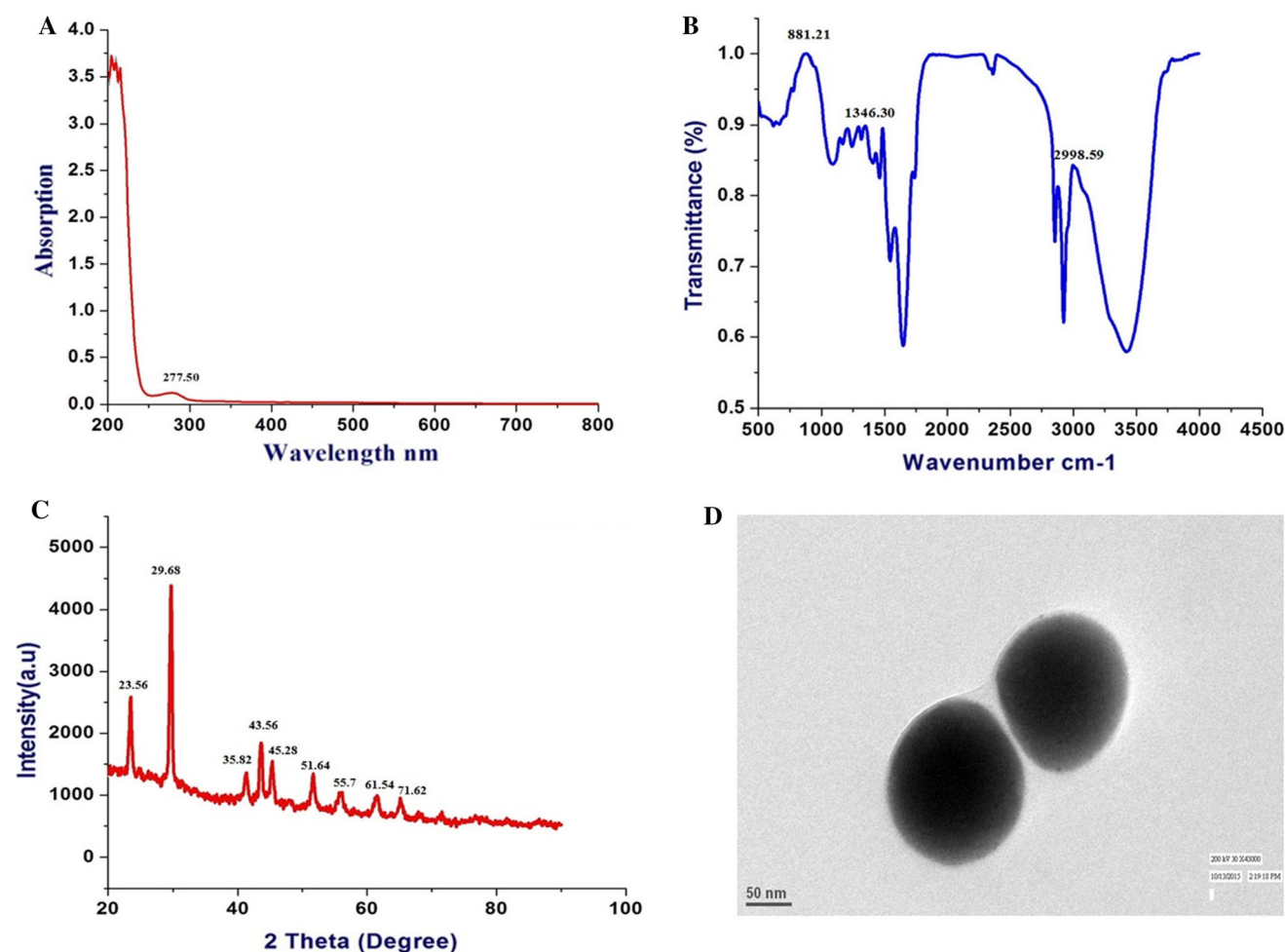


Fig. 1 Characterization of the green synthesized SeNPs **a** UV–Vis analysis **b** FTIR **c** XRD and **d** TEM micrograph

transition from white to yellow is due to the excitation of surface plasmon resonance (SPR) vibrations in the metal nanoparticles. SPR plays a big role in deciding metal NPs optical spectral response and that shifts to a longer wavelength as the particle size increases. The modification of coloring from yellow to pale red may be due to SPR excitation of SeNPs [33]. The FTIR spectrum of SeNP as seen in (Fig. 1b) has vibrational and stretching role at wave numbers with sharp absorption peaks at 881.21 cm^{-1} attributed to C–H aromatics, and the vibration peak at 1346.20 cm^{-1} contributing to the symmetric N–O (Nitro group) stretch. The prominent peaks at 2998.59 cm^{-1} are immensely powerful O–H bond, reflecting carboxylic acid that successfully indicates biosynthesis of SeNPs. Biosynthesized SeNPs was also confirmed by XRD analysis with a clear, sharp and strong representation of the Bragg reflection (Fig. 1c). The Bragg reflection peaks at $2\theta = 23.56, 29.68, 35.82, 43.56, 45.28, 51.64, 55.7, 61.54, 71.62$ and 78.44 refer to the (100), (101), (110), (102), (111), (201), (112), (203), and (210) reflection of pure spherical Se nanoparticles. In addition, the size and morphology of the biosynthesized SeNPs were characterized by TEM micrograph (Fig. 1d) which clearly showed a mono dispersed, uniform spherical shape of nanoparticles with a mean diameter of approximately 70 nm.

The synthesized particle's charge was determined by zeta potential (Fig. 2a) which indicated relatively negative charged nature. The corresponding value of zeta potential was -17.8 mV . As the same charge have the property to repel each other, it provides higher stability to nanoparticles and restricts agglomeration. The hydrodynamic diameter and size distribution of SeNPs was measured by DLS. As shown in Fig. 2b the diameter of SeNPs was 55.9 nm with a polydispersity index (PDI) of 0.03. The Zeta potential greater than $+30$ or less than -30 mV indicates stable dispersion, and null zeta potential implies unstable dispersion. The zeta potential of the SeNPs was located at -17.8 mV and offers the repulsive force as an electrostatic stabilization and because of the phytonutrients and proteins attached to the SeNPs exterior it plays a significant role in stabilizing these dispersions. Previous report indicated a reduced plasma protein adsorption and reduced number of non-specific cellular uptake with negatively charged surface biosynthesized NPs. In the meantime, the charged NPs can repulse each other to resolve the natural propensity of NP aggregation. The synthesizing and stabilizing of NPs thus have sufficient stability of dispersion in aqueous solution and satisfactory for accumulation by EPR effects in the tumor tissue [34, 35].

In Vitro Cytotoxicity

Figure 3 showed the in vitro cytotoxicity potential of SeNPs at different concentrations and its effects on proliferation of MDA-MB-231 cells and HBL-100 cells by MTT assay. This was done to report the cytotoxicity of synthesized SeNPs using *Carica papaya* latex against breast cancer cell line (Scheme 2). In the present study, we investigated that the induction of apoptosis could be the possible mechanism of anti-proliferative activity of biosynthesized SeNPs. SeNPs used varying concentrations (5, 10, 15, 20, 25, 30, 35, 40, 45, and 50 $\mu\text{g/mL}$) to treat MDA-MB-231 cells at 48 h. Fifty percentage of cell death, which determines the inhibitory concentration (IC_{50}) value of biosynthesized SeNPs against MDA-MB-231 cells was found to be 34 $\mu\text{g/mL}$ in 48 h. However, the cytotoxicity assay of biosynthesized SeNPs against HBL-100 did not exhibit significant cytotoxicity at lower concentration and cytotoxicity increases with concentration increasing above 50 $\mu\text{g/mL}$ in 48 h. Our results also provide conclusive evidence for the cytotoxic effect of biosynthesized SeNPs against breast cancer MDA-MB-231 cell line compared with HBL-100 normal breast cell line [36–38]. Most research focuses on the toxicity of NPs consisting of chemical or physical synthesized metal oxide NPs. There are few indications characterizing the nanotoxicity of metal oxide NPs made of biogenic formulation. Consistent evaluation of the similarities and differences of metal oxide NPs acquired by conventional methods and biogenic routes in terms of toxicity can be complex. This complexity is due to different routes of the synthesis of NPs, their different size, existence or lack of capping molecules, different types of toxicity assessment tests, and lack of broader nanotoxicity studies of biogenic NPs. NPs' toxicity is determined largely by their chemical and physical properties, such as shape, size, surface charge, remarkable surface area, catalytic activity and the appearance or unavailability of a shell and energetic surface functional groups [16, 34, 39–41]. Furthermore, the potential damaging effect of NPs depending on their composition, length of their contact with living matter, absorption in biological fluids, and potential for tissue or organ aggregation. Developing safe, biocompatible NPs which can be used for human diagnosis and treatment can only be based on a complete understanding of the connections between all the factors and processes that underlie NP toxicity. Pan et al. identified the toxicity dependency of gold NPs in the range from 0.8 to 15 nm on their thickness. For fibroblasts, epithelial cells, macrophages, and melanoma cells, the NPs 15 nm in size were found to be 60 times lesser toxic than 1.4 nm NPs. It is also worthy of noting that 1 and 4-nm NPs induce cell

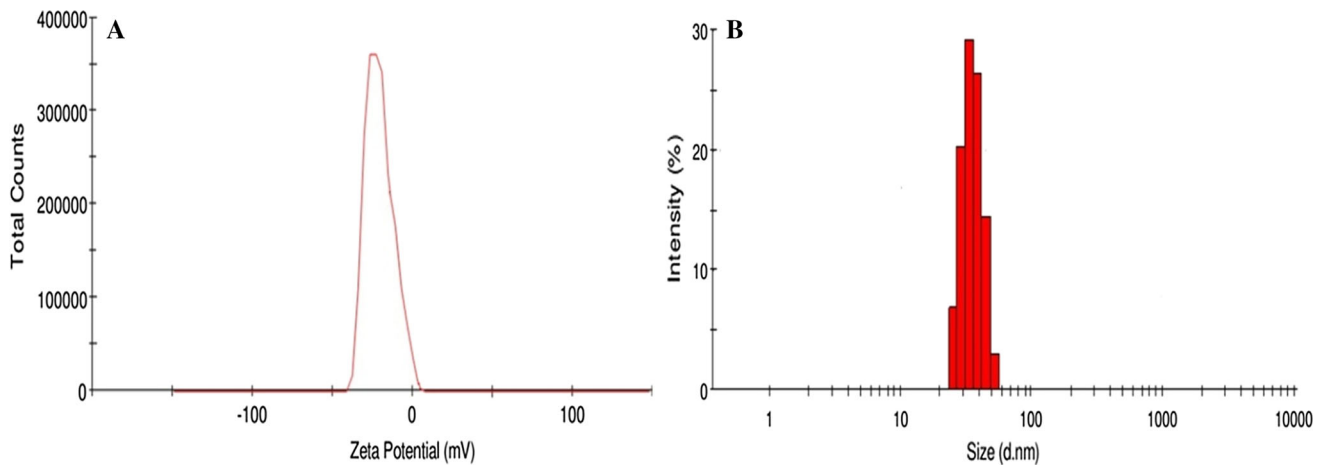


Fig. 2 a Zeta potential measurement b size distribution of biosynthesized SeNPs

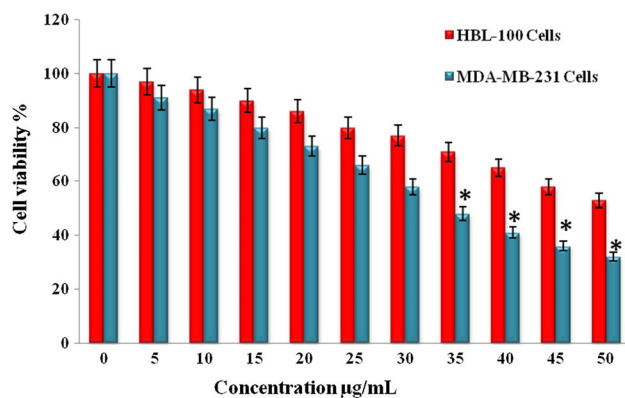


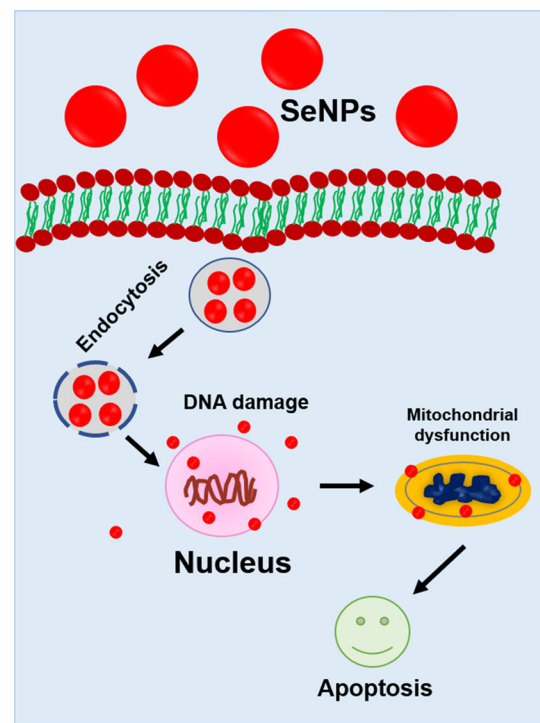
Fig. 3 The MTT assay for relative cell viabilities of the MDA-MB-231 breast cancer cells and HBL-100 normal breast cells incubated with biosynthesized SeNPs for 48 h

necrosis, while 1 and 2-nm NPs induce apoptosis primarily within 12 h [34, 41–44].

Fluorescence Microscopic Studies

AO/EtBr Staining for Detection of Apoptotic Cells

The induction of apoptosis, after the treatment with IC_{50} concentration of SeNPs was assessed by fluorescence microscopy after staining with acridine orange/ethidium bromide (AO/Etbr) as shown in Fig. 4a. Because AO can penetrate the normal cell membrane, the cells were observed as green fluorescence, while apoptotic cells and apoptotic bodies formed as a result of nuclear shrinkage and blebbing were observed as orange colored bodies whereas, necrotic cells were observed as red color fluorescence due to their loss of membrane integrity when viewed under fluorescence microscope [45, 46].



Scheme 2 Mode of entry and their action of biosynthesized SeNPs

DAPI Staining for Nuclear Morphology Study

DAPI is a popular nuclear counter stain and the SeNPs induced nuclear fragmentation was observed by DAPI staining. The untreated cells showed normal nuclei (smooth nuclear) whereas after treatment of MDA-MB-231 cells with SeNPs, the apoptotic nuclei (condensed or fragmented chromatin) were observed as shown in Fig. 4b. Nuclear morphology analysis showed characteristic apoptotic changes, such as chromatin condensation, fragmentation of the nucleus, and formation of apoptotic bodies in the MDA-MB-231 cells. Interestingly, some studies have reported that

Fig. 4 a Fluorescent microscopic images (400 X magnifications) of MDA-MB-231 cells stained with AO/EtBr and DAPI Staining. The AO/EtBr stained cells observed to have (orange) the loss of DJm and the induction of apoptosis. **b** DAPI staining (blue colour) shows the condensed and fragmented nuclear bodies in treated cells compared with untreated (control) cells in MDA-MB-231 cells treated with different formulation of SeNPs for 48 h (color figure online)

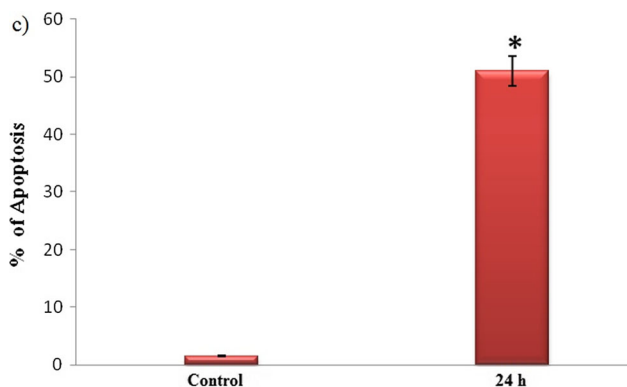
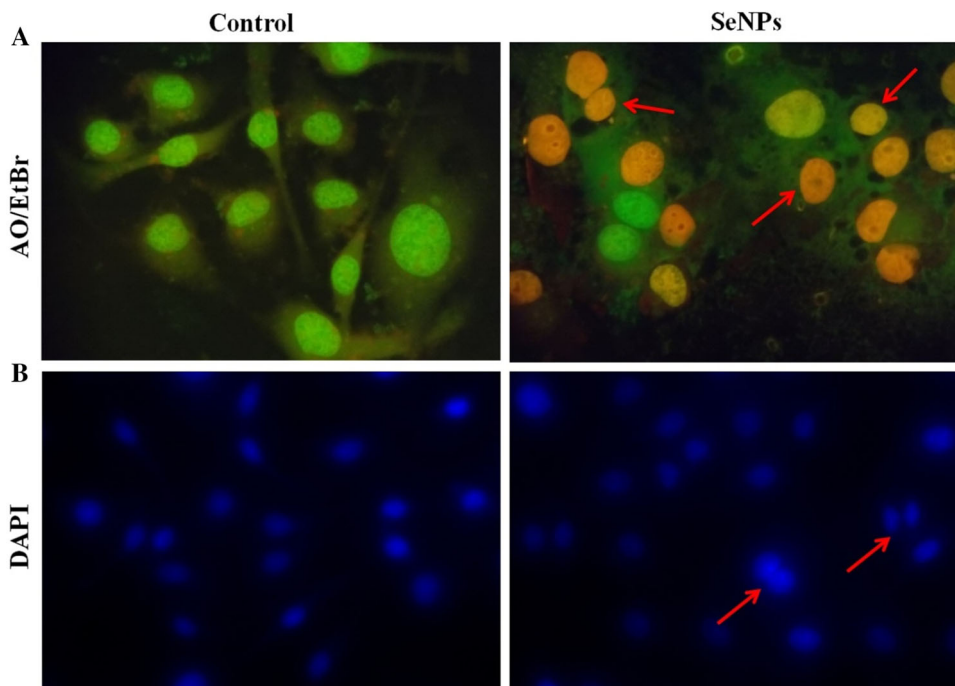


Fig. 5 Percentage of apoptotic cells measured after MDA-MB-231 cells were incubated with IC_{50} concentration of SeNPs. Data represents mean \pm SD * $P < 0.05$ was considered statistically significant

SeNPs can also induce DNA damage and apoptosis in cancer cells. With an increase in concentration of SeNPs, number of apoptotic cells were increased, which suggest that SeNPs could induced cell apoptosis. Figure 5 shows that the total number of apoptotic cells increase when incubation time increases due to nuclear fragmentation as noticed in SeNPs treated MDA-MB-231 cells.

Conclusion

In this study, Selenium nanoparticles were synthesized from the latex of *Carica papaya* collected from the developing green fruits and characterized by UV-Vis

spectroscopy, FTIR, XRD, DLS and TEM. Synthesized Selenium nanoparticles demonstrated significant cytotoxicity in MDA-MB-231 human breast cancer cells and HBL-100 normal breast cell with IC_{50} values of 34 $\mu\text{g/mL}$ and 50 $\mu\text{g/mL}$, respectively at 48 h treatment. In-vivo experiment proved non-toxicity and biocompatibility of SeNPs. Further studies are required to elucidate the precise molecular mechanism involved in cell growth inhibition thereby permitting the use of biosynthesized SeNPs as cancer chemopreventive and/or therapeutic agents.

References

1. M. Saravanan, T. Asmalash, A. Gebrekidan, D. Gebreegziabiher, T. Araya, H. Hilekiros, H. Barabadi, and K. Ramanathan (2018). Nano-medicine as a newly emerging approach to combat human immunodeficiency virus (HIV). *Pharm. Nanotechn.* **6**, (1), 17–27.
2. V. Varadharaj, A. Ramaswamy, R. Sakthivel, R. Subbaiya, H. Barabadi, M. Chandrasekaran, and M. Saravanan (2019). Antidiabetic and antioxidant activity of green synthesized starch nanoparticles: an in vitro study. *J. Clust. Sci.* **30**, (6), 1–10.
3. J. K. Patra, G. Das, L. F. Fraceto, E. V. R. Campos, M. del Pilar Rodriguez-Torres, L. S. Acosta-Torres, L. A. Diaz-Torres, R. Grillo, M. K. Swamy, S. Sharma, and S. Habtemariam (2018). Nano based drug delivery systems: recent developments and future prospects. *J. Nanobiotechnol.* **16**, (1), 71.
4. A. Khatua, E. Priyadarshini, P. Rajamani, A. Patel, J. Kumar, A. Naik, M. Saravanan, H. Barabadi, A. Prasad, B. Paul, and R. Meena (2020). Phytosynthesis, characterization and fungicidal potential of emerging gold nanoparticles using *Pongamia pinnata* leave extract: a novel approach in nanoparticle synthesis. *J. Clust. Sci.* **31**, (1), 125–131.

5. J. Jeevanandam, A. Barhoum, Y. S. Chan, A. Dufresne, and M. K. Danquah (2018). Review on nanoparticles and nanostructured materials: history, sources, toxicity and regulations. *Beilstein J. Nanotechnol* **9**, (1), 1050–1074.
6. H. Barabadi, M. Ovais, Z. K. Shinwari, and M. Saravanan (2017). Anti-cancer green bionanomaterials: present status and future prospects. *Green Chem. Lett. Rev.* **10**, (4), 285–314.
7. A. Khatua, A. Prasad, E. Priyadarshini, A. K. Patel, A. Naik, M. Saravanan, H. Barabadi, B. Paul, R. Paulraj, and R. Meena (2019). Emerging antineoplastic plant-based gold nanoparticle synthesis: a mechanistic exploration of their anticancer activity toward cervical cancer cells. *J. Clust. Sci.* **12**, (16), 1–12.
8. P. Nithya, M. Balaji, A. Mayakrishnan, S. Jegatheeswaran, S. Selvam, and M. Sundrarajan (2020). Biogenic approach for the synthesis of Ag-Au doped RuO₂ nanoparticles in BMIM-PF₆ ionic liquid medium: Structural characterization and its biocidal activity against pathogenic bacteria and HeLa cancerous cells. *J. Mol. Liq.* **310**, 113245.
9. J. Singh, T. Dutta, K. H. Kim, M. Rawat, P. Samddar, and P. Kumar (2018). 'Green' synthesis of metals and their oxide nanoparticles: applications for environmental remediation. *J. Nanobiotechnol.* **16**, (1), 84.
10. I. Virmani, C. Sasi, E. Priyadarshini, R. Kumar, S. K. Sharma, G. P. Singh, R. B. Pachwarya, R. Paulraj, H. Barabadi, M. Saravanan, and R. Meena (2019). Comparative anticancer potential of biologically and chemically synthesized gold nanoparticles. *J. Clust. Sci.* **31**, 867–876.
11. H. Barabadi, H. Vahidi, K. D. Kamali, M. Rashedi, and M. Saravanan (2019). Antineoplastic biogenic silver nanomaterials to combat cervical cancer: a novel approach in cancer therapeutics. *J. Clust. Sci.* **31**, 659–672.
12. D. Sharma, S. Kanchi, and K. Bisetty (2019). Biogenic synthesis of nanoparticles: a review. *Arab. J. Chem.* **12**, (8), 3576–3600.
13. V. K. Bajpai, M. Kamle, S. Shukla, D. K. Mahato, P. Chandra, S. K. Hwang, P. Kumar, Y. S. Huh, and Y. K. Han (2018). Prospects of using nanotechnology for food preservation, safety, and security. *J. Food Drug Anal.* **26**, (4), 1201–1214.
14. S. Jain and M. S. Mehata (2017). Medicinal plant leaf extract and pure flavonoid mediated green synthesis of silver nanoparticles and their enhanced antibacterial property. *Scientific reports* **7**, (1), 1–13.
15. H. Barabadi, B. Tajani, M. Moradi, K. D. Kamali, R. Meena, S. Honary, M. A. Mahjoub, and M. Saravanan (2019). Penicillium family as emerging nanofactory for biosynthesis of green nanomaterials: a journey into the world of microorganisms. *J. Clust. Sci.* **7**, (1), 1–14.
16. P. Boomi, G. P. Poorani, S. Palanisamy, S. Selvam, G. Ramathanan, S. Ravikumar, H. Barabadi, H. G. Prabu, J. Jeyakanthan, and M. Saravanan (2019). Evaluation of antibacterial and anti-cancer potential of polyaniline-bimetal nanocomposites synthesized from chemical reduction method. *J. Clust. Sci.* **30**, (3), 715–726.
17. M. Roman, P. Jitaru, and C. Barbante (2014). Selenium biochemistry and its role for human health. *Metallomics* **6**, (1), 25–54.
18. E. Mocchegiani and M. Malavolta Role of zinc and selenium in oxidative stress and immunosenescence: implications for healthy ageing and longevity. *Handbook on immunosenescence* (Springer, Dordrecht, 2009), pp. 1367–1396.
19. P. R. Hoffmann and M. J. Berry (2008). The influence of selenium on immune responses. *Mol. Nutr. Food Res.* **52**, (11), 1273–1280.
20. B. Hosnedlova, M. Kepinska, S. Skalickova, C. Fernandez, B. Ruttkay-Nedecky, Q. Peng, M. Baron, M. Melcova, R. Opatrilova, J. Zidkova, and G. Bjørklund (2018). Nano-selenium and its nanomedicine applications: a critical review. *Int. J. Nanomed.* **13**, 2107.
21. H. Vahidi, H. Barabadi, and M. Saravanan (2019). Emerging selenium nanoparticles to combat cancer: a systematic review. *J. Clust. Sci.* **31**, 1–9.
22. L. Guo, K. Huang, and H. Liu (2016). Biocompatibility selenium nanoparticles with an intrinsic oxidase-like activity. *J. Nanopart. Res.* **18**, (3), 74.
23. W. Chen, Y. Li, S. Yang, L. Yue, Q. Jiang, and W. Xia (2015). Synthesis and antioxidant properties of chitosan and carboxymethyl chitosan-stabilized selenium nanoparticles. *Carbohydr. Polym.* **132**, 574–581.
24. Y. Huang, L. He, W. Liu, C. Fan, W. Zheng, Y. S. Wong, and T. Chen (2013). Selective cellular uptake and induction of apoptosis of cancer-targeted selenium nanoparticles. *Biomaterials* **34**, (29), 7106–7116.
25. L. Guo, J. Xiao, H. Liu, and H. Liu (2020). Selenium nanoparticles alleviate hyperlipidemia and vascular injury in ApoE-deficient mice by regulating cholesterol metabolism and reducing oxidative stress. *Metallomics* **2020**, (12), 204–217.
26. H. Barabadi, B. Tajani, M. Moradi, K. D. Kamali, R. Meena, S. Honary, M. A. Mahjoub and M. Saravanan (2019). Penicillium family as emerging nanofactory for biosynthesis of green nanomaterials: a journey into the world of microorganisms. *J. Clust. Sci.* pp.1-14.
27. A. Ali, S. Devarajan, M. Waly, M. M. Essa, and M. S. Rahman *Nutritional and medicinal value of papaya (Carica papaya L.). Natural products and bioactive compounds in disease prevention* (Nova Science Publishers, New York, 2011), **18**, 307–324.
28. P. Chávez-Quintal, T. González-Flores, I. Rodríguez-Buenfil, and S. Gallegos-Tintoré (2011). Antifungal activity in ethanolic extracts of Carica papaya L. cv. Maradol leaves and seeds. *Indian J. Microbiol.* **51**, (1), 54–60.
29. T. Viji and Y. Prashar (2015). A review on medicinal properties of Carica papaya Linn. *Asian Pac. J. Trop. Dis.* **5**, (1), 1–6.
30. C. Murugan, K. Rayappan, R. Thangam, R. Bhanumathi, K. Shanthi, R. Vivek, R. Thirumurugan, A. Bhattacharyya, S. Sivasubramanian, P. Gunasekaran, and S. Kannan (2016). Combinatorial nanocarrier based drug delivery approach for amalgamation of anti-tumor agents in breast cancer cells: an improved nanomedicine strategy. *Sci. Rep.* **6**, (1), 1–22.
31. C. Murugan, S. Venkatesan, and S. Kannan (2017). Cancer therapeutic proficiency of dual-targeted mesoporous silica nanocomposite endorses combination drug delivery. *ACS omega* **2**, (11), 7959–7975.
32. K. Rayappan, C. Murugan, S. Sundarraj, R. P. Lara, and S. Kannan (2017). Peptide-conjugated nano-drug delivery system to improve synergistic molecular chemotherapy for colon carcinoma. *ChemistrySelect* **2**, (27), 8524–8534.
33. H. Barabadi, S. Honary, P. Ebrahimi, A. Alizadeh, F. Naghibi, and M. Saravanan (2019). Optimization of myco-synthesized silver nanoparticles by response surface methodology employing Box-Behnken design. *Inorg. Nano-Metal Chem.* **49**, (2), 33–43.
34. H. Barabadi, S. Honary, M. A. Mohammadi, E. Ahmadpour, M. T. Rahimi, A. Alizadeh, F. Naghibi, and M. Saravanan (2017). Green chemical synthesis of gold nanoparticles by using Penicillium auleatum and their scolicidal activity against hydatid cyst protoscolices of *Echinococcus granulosus*. *Environ. Sci. Pollut Res.* **24**, (6), 5800–5810.
35. S. Rajasekar, E. M. Martin, S. Kuppusamy, and C. Vetrivel (2019). Chitosan coated molybdenum sulphide nanosheet incorporated with tantalum oxide nanomaterials for improving cancer photothermal therapy. *Arab. J. Chem.* **3**, 4741–4750.
36. C. Murugan, N. Murugan, A. K. Sundramoorthy, and A. Sundaramurthy (2019). Nanoceria decorated flower-like molybdenum sulphide nanoflakes: an efficient nanozyme for tumour

- selective ROS generation and photo thermal therapy. *Chem. Commun.* **55**, (55), 8017–8020.
37. K. Liu, P. C. Liu, R. Liu, and X. Wu (2015). Dual AO/EB staining to detect apoptosis in osteosarcoma cells compared with flow cytometry. *Med. Sci. Monit Basic Res.* **21**, 15.
38. S. Kasibhatla, G. P. Amarante-Mendes, D. Finucane, T. Brunner, E. Bossy-Wetzel, and D. R. Green (2006). Acridine orange/ethidium bromide (AO/EB) staining to detect apoptosis. *Cold Spring Harbor Protoc.* **2006**, (3), pdb-prot4493.
39. H. Barabadi, O. Hosseini, K. D. Kamali, F. J. Shoushtari, M. Rashedi, H. Haghi-Aminjan and M. Saravanan (2019). Emerging theranostic silver nanomaterials to combat lung cancer: a systematic review. *J. Clust. Sci.* pp.1–10.
40. S. Honary, H. Barabadi, E. Gharaei-Fathabad, and F. Naghibi (2013). Green synthesis of silver nanoparticles induced by the fungus *Penicillium citrinum*. *Trop. J. Pharm. Res.* **12**, (1), 7–11.
41. H. Barabadi, M. A. Mahjoub, B. Tajani, A. Ahmadi, Y. Junejo, and M. Saravanan (2019). Emerging theranostic biogenic silver nanomaterials for breast cancer: a systematic review. *J. Clust. Sci.* **30**, (2), 259–279.
42. S. Honary, H. Barabadi, P. Ebrahimi, F. Naghibi, and A. Alizadeh (2015). Development and optimization of biometal nanoparticles by using mathematical methodology: a microbial approach. *J. Nano Res.* **30**, 106–115.
43. H. Barabadi (2017). Nanobiotechnology: a promising scope of gold biotechnology. *Cell. Mol. Biol* **63**, 3–4.
44. M. T. Rahimi, E. Ahmadpour, B. R. Esboei, A. Spotin, M. H. K. Koshki, A. Alizadeh, S. Honary, H. Barabadi, and M. A. Mohammadi (2015). Scolicidal activity of biosynthesized silver nanoparticles against *Echinococcus granulosus* protoscolices. *Int. J. Surg.* **19**, 128–133.
45. E. Nagaraj, K. Karuppanan, P. Shanmugam, and S. Venugopal (2019). Exploration of bio-synthesized copper oxide nanoparticles using *Pterolobium hexapetalum* leaf extract by photocatalytic activity and biological evaluations. *J. Clust. Sci.* **30**, (4), 1157–1168.
46. N. Elavarasan, K. Kokila, G. Inbasekar, and V. Sujatha (2017). Evaluation of photocatalytic activity, antibacterial and cytotoxic effects of green synthesized ZnO nanoparticles by *Sechium edule* leaf extract. *Res. Chem. Intermed* **43**, (5), 3361–3376.

Publisher's Note Springer Nature remains neutral with regard to jurisdictional claims in published maps and institutional affiliations.